# TWENTY-EIGHT-ELEMENT FUEL-CHANNEL THERMAL-CHEMICAL EXPERIMENTS

P.J. MILLS, D.B. SANDERSON, K.A. HAUGEN, AND G.G. HAACKE

AECL Whiteshell Laboratories
Pinawa, Manitoba, Canada R0E 1L0
(204)753-2311

## ABSTRACT

*Three 28-element out-of-pile fuel-channel experiments have been performed to provide validation and assessment data for various high-temperatures fuel-channel codes and to further the understanding of CANDU® fuel channel behaviour under severe accident conditions. The test section in these experiments consisted of a 28-element bundle of fuel-element-simulators surrounded by a reactor grade pressure tube mounted inside a Zr-2 calandria tube. During the experiment, high-temperature steam was heated by the electrically heated fuel element simulators until the steam and zirconium surfaces in the test section were at sufficient temperatures to initiate the exothermic zirconium-steam reaction. The fuel element simulators were powered until simulator temperatures reached 1700°C then power was turned to zero. Analysis of experimental results indicated the exothermic zirconium-steam reaction within the channel was locally self-sustaining as fuel element simulator temperatures increased to values as high as 1950°C and up to 57 moles of hydrogen were produced in the test section prior to shutting down the experiment.*

## 1. INTRODUCTION

In a CANDU® Pressurized Heavy-Water (PHW) reactor, the fuel and coolant are separated from the heavy-water neutron moderator by horizontal fuel channels. The fuel channel consists of a Zr-2.5 Nb pressure tube and a Zircaloy-2 calandria tube, separated by a gas-filled annulus. It is important to have a thorough understanding of high-temperature fuel-channel behaviour and to know the effectiveness of the moderator as a heat sink to demonstrate the safety of current and future CANDU PHW reactors during postulated accidents.

This understanding is best achieved by studying the underlying phenomena using mathematical models and single-effect tests. These models are then coupled into an integrated code to predict fuel-channel behaviour under accident conditions. Computer codes such as CHAN-II [1], CATHENA [2] and FACTAR [3] are capable of predicting the thermal-chemical response of CANDU fuel channels when the internal coolant is superheated steam. These codes, however, must be validated against experimental data whenever possible. Data for validation of the codes come from various integrated experiments involving the complex interaction of temperature, material properties, heat transfer and reaction kinetics on fuel-channel components subjected to severe temperature transients. The integrated experiments described in this paper provide a database to be used for validating fuel-channel codes.

The methodology adopted in the CHAN Thermal-Chemical experimental program has been to perform several series of experiments, progressing from a single fuel element simulator (FES), to seven elements and finally to 28-element geometries. The single and seven-element series have been completed and reported [Ref. 4-6].

This paper summarizes the results from the third and final 28-element experiment, CS28-3, and compares the results from this experiment to the results from the two preceding 28-element experiments, CS28-1 and CS28-2.

CANDU® is a registered trademark of Atomic Energy of Canada Limited (AECL)

## 2. MATERIALS AND METHODS

### 2.1 Experimental Apparatus

Figure 1 illustrates the test apparatus used for the CS28-3 experiment. The same test apparatus was used for all three 28-element experiments with some variation in the design of the test section. The calandria tube was surrounded by an open tank of water during the first two experiments (CS28-1 and CS28-2) to provide reactor-typical cooling on the calandria tube surface. A cooling water jacket (CWJ) was used in place of the open tank in CS28-3 to remove the uncertainties in determining the radial heat flow from the FES bundle to the outer surface of the calandria tube.

Experiments CS28-1 and CS28-3 used a reactor-typical pressure tube in the test section. The CS28-2 experiment used a partially ballooned pressure tube to study the fuel channel behaviour when the majority of the steam flow in the test section bypassed the FES bundle.

During the 28-element experiments, superheated steam at 700°C entered the test section from the steam superheater. In the test section, the 28 fuel element simulators raised the temperature of the steam and zirconium surfaces to temperatures sufficient to cause the zirconium and steam to react. The reaction produced hydrogen gas and energy which further raised surface temperatures and increased the reaction rate. The steam and hydrogen gas mixture left the test section and flowed into the condenser where the steam was condensed. The hydrogen gas was separated from the water in a water trap, dried in water filters, measured by a mass flow meter and vented to atmosphere.

The 28-element FES bundle (Figure 2) was surrounded by a 2330-mm long section of autoclaved Zr-2.5 Nb pressure tube mounted inside a 2030-mm long Zr-2 calandria tube. The test-section annulus (gap between the pressure and calandria tubes) contained one Zr-Nb-Cu garter spring located at the test-section axial centreline.

The FES bundle consisted of three rings of FESs concentrically located inside the pressure tube. Each FES consisted of a 6-mm diameter graphite rod heater (1800 mm in length) inside annular alumina pellets (14.30-mm OD, 6.20-mm ID and 16 mm in length) in a Zr-4 fuel-sheath.

Five spacer plates were evenly distributed along the heated length of the FES bundle. The purpose of the spacer plates was to simulate the effects of CANDU bundle appendages (end plates, spacer pads and bearing pads) on the steam flow in the FES bundle, and to help minimize sag of the FESs at high temperatures.

### 2.2 Instrumentation

The FESs were connected in parallel to a 5000 A dc power supply. The FES power connections were set up in three distinct rings: inner, middle and outer (R1, R2 and R3 respectively in Figure 2). This allowed the radial power distribution in the FES bundle to approximate the profile found in a typical CANDU 28-element bundle.

The FES bundle was radially subdivided into six rings for thermocouple installation (Figure 2). The FES thermocouples had 0.25-mm diameter C-type (W-5% Re/W-26% Re) sensing elements threaded through double bore alumina insulators inside a 1.55-mm diameter tantalum sheath. The tantalum sheaths were threaded through holes in the alumina pellets in the FESs. The sensing end of the thermocouple was estimated to be 1.84 mm from the FES outside surface.

The thermocouples on the pressure-tube outer surface were magnesium oxide (MgO) insulated R-type (platinum-rhodium) thermoelements inside 1-mm outer diameter Inconel sheaths. The individual wires were slightly separated and spot-welded directly to the surface of the pressure tube. The thermocouples on the calandria-tube outer surface were fiberglass-insulated K-type (chromel-alumel) with 0.13-mm diameter sensing elements. The separated sensing wires were spot welded directly onto the calandria-tube surface.

Seven C-type thermocouples were installed in the FES bundle subchannels (two at the inlet end and five at the outlet end) to measure the inlet and outlet steam temperatures. The sensing end of the thermocouples was surrounded by a radiation shield to reduce radiative heat transfer from the adjacent FESs.

Resistance temperature detectors were used to measure the water temperature in the open tank during experiments CS28-1 and CS28-2 and the water temperatures entering and leaving the cooling water jacket during CS28-3.

Steam flow to the test section inlet was determined using an orifice plate and pressure measurements were made using Rosemount pressure transmitters.

Hydrogen production was monitored by two mass flow meters to preserve accuracy at the low and high hydrogen flow rates expected. The first flow meter was rated for hydrogen flow rates of 0 to 200 standard liters per minute (SLPM) and the second for flows of 0 to 1000 SLPM.

The best-estimate uncertainties in the above instruments is as follows: electric power ±4.38%, pressure (up to 500 kPa) ±0.25%, temperature (up to 2000°C) ±1.23%, steam flow at 10 g/s ±2%, $H_2$ flow (up to 1000 SLPM) ±1.05%, water temperature and flow (CS28-3) ±1.3% and ±0.45% respectively.

### 2.3 Experimental Procedures

The experiments were generally conducted in three stages, a low-power, a high-power and a no-power stage. During the low-power stage, the apparatus was purged with helium, steam flow established and power raised to 10 kW. Stage 1 lasted until the experimenters were satisfied that a quasi-steady state condition existed. At the end of Stage 1, power was raised to full power (130 kW-135 kW) to start Stage 2. Power was held at this value until FES temperatures exceed 1700°C and the electric power was turned off to start Stage 3. Electric power was turned off for Stage 3 to study the energy release from the zirconium-steam reaction. Stage 3 was terminated by shutting off the steam flow when the reaction rates and test-section temperatures decreased.

## 3. RESULTS

### 3.1 Detailed Results From the CS28-3 Experiment

Table 1 summarizes the key operating conditions and results of the CS28-3 experiment. Figure 3 shows the key transient system parameters during the experiment.

Stage 1 of the CS28-3 experiment included all operation from first start up to the low-power steady-state operation at 10 kW power. Stage 1 ended at t=1067 s, when power was raised to 130 kW to start the high temperature transient. Superheated steam (at 700°C) was supplied to the test section at 9 g/s throughout the high temperature transient (Stage 2 and 3). The nominal pressure in the test section remained below 180 kPa (abs) throughout the experiment.

Minimum and maximum test-section outlet temperatures of the steam recorded by the five in-bundle thermocouples at the time of peak test-section temperatures were 1790°C and 1610°C respectively. The steam temperature measurement in the steam outlet line at this time was 1275°C. The lower temperature in the steam outlet line reflects the cooler steam temperatures in the outer flow area between the outer ring of FESs and the pressure tube as well as heat losses by the steam to the water cooled end fittings and the surroundings. All test-section outlet steam thermocouple measurements were used to determine an average test-section outlet temperature for energy balance calculations. Each thermocouple reading was weighted according to the portion of fluid it was assumed to represent. The weighted-average steam outlet temperature peaked at 1520°C during the experiment.

Water at 23°C was pumped to the cooling water jacket surrounding the calandria tube at a rate of approximately 355 g/s. The inside surface of the cooling water jacket was equipped with vanes to direct the cooling water flow in a spiral motion around the calandria tube. The spiral motion of the coolant ensured good mixing of the cooling water and a high heat transfer coefficient on the calandria-tube surface. The maximum recorded temperature of the cooling water jacket exit flow was 66°C.

During Stage 2 electric power to the FES bundle remained near 130 kW until peak FES temperatures reached 1700°C. At t=1384.5 s electric power to the FES bundle was turned to zero to study the energy released from the

exothermic zirconium-steam reaction. The measured normalized powers for the inner, middle and outer ring FESs were 0.744, 0.880 and 1.123 respectively during the high power stage.

Figure 4 illustrates the hottest FES temperatures recorded during the experiment. The figure indicates the hottest surfaces were on the inside surfaces of the Ring-1 simulators. The average rate of temperature increase of all FES thermocouples during Stage 2 was 2.5 °C/s. The rate of temperature rise increased when temperatures exceeded 1550 °C due to the increase in the zirconium-steam oxidation rate. The FES temperature at which the rate of increase changed was not the same for all thermocouples. The majority of the FES-temperature traces show the rate change around 1550 °C but for some thermocouples the change occurred at temperatures as low as 1525 °C or as high as 1575 °C. Thermocouple TC30 recorded the greatest rate of temperature increase (4.6 °C/s) when FES temperatures exceeded 1550 °C. This change in heatup rate is indicative of the step change in the zirconium-steam oxidation rates due to changes in the structure of zirconium oxide from tetragonal to cubic.

Some FES temperatures continued to increase for 125 s after electric power to the FES bundle was turned off. The temperature increase in the FES bundle, after electric power was turned to zero, confirms the exothermic zirconium-steam reaction was locally self-sustaining. Peak recorded FES temperatures during Stage 3 were 1870 °C and 1860 °C on TC30 and TC37 respectively. These thermocouples increased 239 °C and 125 °C respectively in the first 50 s after electric power was turned to zero.

The TC30 and TC37 temperature traces show a drop in measured temperatures followed by a subsequent temperature increase. This is indicative of steam starvation at those locations. Fuel element simulator sheath temperatures decreased when there was not enough steam to fuel the exothermic zirconium-steam reaction and rapidly increased again once steam became available to that location.

Figure 5 shows the hottest pressure-tube temperatures recorded during the experiment. The temperature increase of the pressure tube during Stage 2 was uniform in the axial as well as the circumferential directions. Most thermocouples experienced a temperature increase in the range 1.7 °C/s to 2.2 °C/s. Thermocouple TC62 located near the centre of the test section (825 mm into the heated zone or Z=825 mm) experienced a temperature increase of 2.4 °C/s during Stage 2.

Pressure-tube temperatures continued to increase for 80 to 100 s after electric power to the FES bundle was turned off. Most thermocouples recorded temperature increases between 80 °C and 100 °C during Stage 3. The temperature increase in the pressure tube after power was turned to zero reflects the continued increase in FES temperatures as a result of the locally self-sustaining exothermic zirconium-steam reaction. The highest pressure-tube temperature recorded during the experiment was 1436 °C recorded by thermocouple TC62, 825 mm into the heated zone.

The bottom of the pressure tube registered higher temperatures because sagging of the FES bundle narrowed the separation between the hot FESs and the pressure tube and therefore increased heat transfer to the bottom of the pressure tube by conduction and radiation. The sagging FES bundle also reduced the steam flow and thus the heat removal by the steam along the bottom of the pressure tube.

Figures 6 shows the two hottest calandria-tube temperatures along the test section. Calandria-tube temperatures increased from their low power (Stage 1) steady state values of 23 to 49 °C to above 100 °C during Stage 2. This increase in calandria-tube surface temperature is a reflection of the increase in radial heat transfer from the FES bundle to the cooling water jacket flow as test section temperatures increased. The peak recorded calandria-tube temperature during the experiment was 127 °C (TC89) along the bottom of the tube, 825 mm into the heated zone. A number of calandria-tube temperatures exhibited a temperature plateau during Stage 3. This plateau indicates the surface of the calandria tube was in the subcooled boiling heat transfer regime.

Hydrogen production from the zirconium-steam reaction started at t=1100 s when maximum measured FES temperatures in the test section were at 800 °C (Figure 7). The hydrogen production rate increased slowly until t=1200 s at which time maximum measured FES temperatures were 1090 °C. The hydrogen production rate

changed to its highest rate of rise at t=1365 s. At this point in time there were 17 thermocouples in the test section recording temperatures greater than 1525 °C. The highest thermocouple reading was 1617 °C (TC37) and the average temperature of the 17 thermocouples was 1560 °C. The hydrogen production rate at the end of Stage 2 reached 0.31 moles/s.

The hydrogen production rate continued to increase after electric power to the test section was shut off, reaching 0.394 moles/s at t=1409 s. The continued increase in the hydrogen production rate during the early part of Stage 3 confirms the zirconium-steam reaction was locally self-sustaining for 23 s under these experimental conditions. The fact that the escalation did not continue beyond t=1409 s, however, is indicative of the fact that globally, the energy production from the zirconium-steam reaction alone was not enough to keep the test section temperatures increasing. A total of 54.3 moles of hydrogen were produced during the experiment.

The components of the test-section energy balance are shown in Figure 8. Heat was generated by the electric current flowing through the graphite heaters in the FES bundle and by the exothermic zirconium-steam reaction. Part of this heat was stored in different components of the apparatus as sensible heat, and part was removed by the steam flow and the cooling water jacket flow. The largest component was removed by the cooling water jacket flow. Heat losses to the end connections could not be determined for our apparatus but were estimated to be a low percentage of the total energy input.

The electric power supplied to the FES bundle was constant at 130 kW during Stage 2 and was turned to zero at t=1385 s. The energy into the test section from the zirconium-steam reaction is a linear function of the measured hydrogen flow rate so its trace resembles the trace shown in Figure 7.

The energy removed by the steam flow was the product of the mass flow of steam entering the test section, the specific heat of the steam at the average steam temperature and the change in steam temperature as it flowed through the test section ($Q_{steam} = \dot{M} \cdot Cp \cdot \Delta T|_{steam}$). The trace of the energy removed by the steam goes to zero at t=1546 s when the steam flow to the test section was turned off.

The radial heat transfer through the pressure-tube/calandria-tube wall to the cooling-water-jacket flow was determined using two different algorithms. The first algorithm determined the heat removed by the cooling water jacket flow similar to the $Q_{steam}$ calculation ($Q_{water}$). The second algorithm determined the radial heat transfer by calculating conduction and radiation heat transfer through the $CO_2$ gas annulus using measured pressure-tube and calandria-tube temperatures.

The total radial heat transfer determined by these two algorithms yield similar energy traces but are offset in time by approximately 63 s. The heat removed by the water ($Q_{water}$) peaked to 63.7 kW at t=1528 s. The heat transferred across the pressure-tube/calandria-tube gap ($Q_{gap}$) peaked to 64.6 kW at 1465 s. The time shift is reasonable given that the determination of $Q_{water}$ is dependent on the outlet temperature measurement and that in turn is dependent on the transit time of the cooling water jacket flow. The calculated heat flow across the $CO_2$ gap ($Q_{gap}$) was used in the energy balance calculations.

The overall energy balance for the CS28-3 experiment is shown in Figure 9. At the time electric power to the FES bundle was turned to zero, the energy produced by the zirconium-steam reaction exceeded the estimated heat removal from the test section by 17 kW. As a result, test-section temperatures continued to increase and the zirconium-steam reaction was locally self-sustaining. The energy produced by the zirconium-steam reaction increased at a greater rate than the energy removal for 23 s and the energy into the test section peaked for the last time at 115.4 kW (t=1408 s). The energy from the chemical reaction remained greater than the energy removed from the test section for another 37 s. The shaded area in Figure 9 shows the period of time the energy from the zirconium-steam reaction exceeded the estimated heat removal from the test section.

The pressure tube was potted with epoxy prior to disassembling the test section to "freeze" the FES bundle in place, such that any bundle deformation could be documented. Once potted, the calandria tube was cut off and measurements taken on the pressure tube. The maximum pressure-tube sag was 7.9 mm, 1185 mm into the heated zone. The overall change in the axial length of the pressure tube due to oxidation growth was 7 mm.

The test section was then sectioned at several axial locations to determine FES bundle deformation and to obtain samples for metalographic examination. Pressure-tube samples were also taken to determine their dissolved hydrogen concentrations as part of the post-test evaluation. The maximum pressure-tube hydrogen concentration was 26 $\mu$g/g on the bottom of the pressure tube, 1725 mm into the heated zone.

The maximum oxide thickness on the FES samples was on the inner facing surface of the third FES in the outer ring (R3-3i in Figure 2) 1425 mm into the heated zone. The oxide thickness at this location was 0.414 mm, which translates to 62% of the original zirconium sheath being oxidized. The oxide thicknesses on the FES sheath opposite the two hottest thermocouple measurements in the test section were 0.336 mm (TC30, 50% of original sheath) and 0.376 mm (TC37, 56.3% of original sheath). The average zirconium consumption of the 48 FES sheath samples was 35%.

The maximum oxide thickness on the inside surface of the pressure tube was 0.0754 mm. This measurement implies approximately 1% of the pressure-tube wall was oxidized at this location.

## 3.2 Overview of the 28-Element Experiments

Three, 28-element high-temperature fuel-channel experiments have been successfully completed and have provided a valuable data base for code validation [7,8]. Figure 10 illustrates the cross section of each test-section used in this series of experiments. The FES bundle geometry and component materials were the same for each experiment. The maximum measured hydrogen production rates and FES temperatures for each experiment are also shown on Figure 10. The temperature and hydrogen production traces in the figure are shifted in time so the peak measured value for each experiment is shown to occur at the same time. Some key experimental results from the three experiments are tabulated in Table 2.

CATHENA was used to perform pre-test simulations for each experiment to determine the steam flow rate that would maximize the length of the zirconium-steam reaction. The steam flow rate for the CS28-2 experiment was much higher than the other two experiments because the partially ballooned pressure tube allowed much of the steam to bypass the FES bundle. Flow to the CS28-1 test section was stopped shortly after power to the FES bundle was turned to zero. This action was necessary because a mechanical failure at the test-section outlet presented a safety hazard. The premature termination of the experiment resulted in lower FES temperatures and hydrogen production.

In all three experiments, energy released from the zirconium-steam reaction did not become significant until FES temperatures exceeded 1200°C. The energy produced by the reaction must exceed the combined heat removal rate of the steam flow and the water cooling to be self sustaining when the electric power was returned to zero. This was indeed the case in all three experiments and the zirconium-steam reaction was locally self sustaining for up to 23 s. Globally, however, the energy removal from the test sections was sufficient to turn temperatures around and the reaction rates and hydrogen production started to decrease.

Experiment CS28-3 achieved the highest rate of hydrogen generation but overall, more moles of hydrogen were produced during the CS28-2 experiment (Figure 10). The amount of oxidation that occurred on the FES sheath material was also greater during the CS28-2 experiment. On average 45% of the original sheath material was oxidized during the experiment and a number of samples were completely oxidized.

The greatest sheath temperature was 1950°C during the CS28-2 experiment. This maximum temperature was previously discounted as a valid temperature [8] but is now considered an accurate temperature reading. The decrease in temperature after the first temperature peak is believed to be caused by steam starvation at that location and the second temperature excursion is believed to be caused by the recirculation of fresh steam to the location and an increase in the zirconium-steam reaction. This pattern exists on a number of FES temperature traces.

The horizontal bar superimposed on the temperature plot in Figure 10 indicates the temperature range over which the rate of temperature rise of the FESs change. All three temperature traces show a slope change in the temperature range 1525 °C to 1575 °C. The slope change was due to a phase change in zirconium oxide from a tetragonal to a cubic structure [7]. The diffusion rate of oxygen in cubic zirconium oxide is much greater than in tetragonal zirconium oxide therefore the oxidation rate increases and the rate of temperatures rise also increases.

## 4. SUMMARY

Three 28-element out-of-pile fuel-channel experiments have been performed to provide validation and assessment data for fuel channel codes. This data will be used to assess the radiation, conduction, convection and oxidation models within fuel-channel codes like CHAN-II, FACTAR and CATHENA for multi-ring geometries.

The experiments were successful in obtaining maximum FES temperatures between 1730 and 1950 °C, well above the melting point (1765 °C) of unoxidized Zr-4 sheath material.

Hydrogen production from the exothermic zirconium-steam reaction started when FES temperatures were 800 °C and escalated when the temperatures exceeded 1200 °C indicative of the parabolic oxidation rate of Zr-4 with temperature. Up to 57 moles of hydrogen were produced in the 1800-mm long test-section.

These experiments have also provided a valuable data base for understanding fuel channel behaviour under severe accident conditions.

## REFERENCES


(1) BAYOUMI, M.H., MUIR, W.C. and KUNDURPI, P.S., "Post-Test Simulation of the First CHAN 28-Element Experiment (Verification of CHAN-II MOD 6 Against Experiment)," Presented at the 4th Int. Conf. on Simulation Methods in Nuclear Engineering, Montreal, PQ, 1993 June.

(2) RICHARDS, D.J., HANNA, B.N., HOBSON, N. and ARDRON, K.H., "CATHENA: A Two-Fluid Code for CANDU LOCA Analysis, (renamed from ATHENA)," Presented at the Third Int. Topical Mtg. on Reactor Thermalhydraulics, Newport, RI, 1985 October.

(3) WESTBYE, C.J., BRITO, A.C., MACKINNON, J.C., SILLS, H.E. and LANGMAN, V.J., "Development, Verification and Validation of the Fuel Channel Behaviour Computer Code FACTAR," Proceedings of the 16th Annual CNS Conference, Saskatoon, SK, 1995 June.

(4) BAYOUMI, M.H., MUZUMDAR, A.P., TRAN, F.B.P., LOCKE, K.E., "CHAN-II(MOD 6) Further Verification Against Single and Seven Element Experiments," Proceedings of the 11th Annual CNS Conference, Toronto, ON, pp. 4.14-4.22, 1990 June.

(5) LEI, Q.M., SANDERSON, D.B., BROWN, M.J., and ROSINGER, H.E., "Comparison of CHAN-II-WL Predictions with Measurements Made During Seven-Element High-Temperature Thermal-Chemical Experiments," Presented at the 12th Annual CNS Conference, Saskatoon, SK, 1991 June.

(6) SANDERSON, D.B., HAUGEN, K.A., MOYER, R.G., and ROSINGER, H.E., "Out-of-Pile Fuel Channel Experiments for Severe Accident Conditions," Proceedings of the American Nuclear Society Intl. Topical Mtg. on Safety of Thermal Reactors, Portland, OR, pp. 92-100, 1991 July.

(7) LEI, Q.M., SANDERSON, D.B., HAUGEN, K.A., and ROSINGER, H.E., "Post-Test Analysis of the 28-Element High-Temperature Thermal-Chemical Experiment CS28-1," Presented at the 4th Int. Conf. on Simulation Methods in Nuclear Engineering, Montreal, PQ, 1993 June.

(8) BAYOUMI, M.H., and MUIR, W.C., "Post-Test Simulation and Analysis of the Second Full-Scale CHAN 28-Element Experiment (Validation of CHAN-II (MOD 6) Against Experiments)," Proceedings of the 16th Annual CNS Conference, Saskatoon, SK, 1995 June.

TABLE 1

KEY OPERATING CONDITIONS AND RESULTS OF THE CHAN CS28-3 THERMAL CHEMICAL EXPERIMENT

| Nominal System Parameters | Pressure kPa (abs) | Flow g/s | Temperature °C inlet | outlet,max |
|---|---|---|---|---|
| Steam | 100-175 | 9 | 700 | 1520 |
| Cooling Water Jacket | 90-185 | 355 | 23 | 66 |

| Maximum Temperatures | Thermocouple | Location | Temperature | Time |
|---|---|---|---|---|
| Fuel Element Simulators | TC30 | B11:R1-4i | 1870°C | 1435 s |
| | TC37 | B12:R1-1i | 1860°C | 1439 s |
| | TC38 | B12:R1-2i | 1839°C | 1450 s |
| Pressure Tube | TC62 | P6-C | 1436°C | 1455 s |
| | TC69 | P10-C | 1372°C | 1462 s |
| | TC77 | P12-B | 1370°C | 1467 s |
| Calandria Tube | TC89 | C6-C | 127°C | 1374 s |
| | TC94 | C11-A | 123°C | 1470 s |

- Maximum Hydrogen Generation Rate: 0.394 moles/s, 530 SLPM
  Total Hydrogen Production: 54.3 moles
- Duration of Locally Self-Sustained Zirconium/Steam Reaction 23 s
- Maximum Pressure Tube Hydrogen Concentration at P-12C 26 μg/g
- Maximum Oxide Thickness Location Thickness mm
  Fuel Element Simulators B10:R3-3i 0.414
  Pressure Tube P8-A 0.075

TABLE 2

KEY EXPERIMENTAL RESULTS FROM THE 28-ELEMENT EXPERIMENTS

| | CS28-1 | CS28-2 | CS28-3 |
|---|---|---|---|
| Steam Flow, g/s | 10.2 | 15.0 | 9.0 |
| Self Sustaining Zr/Steam Reaction | Yes(15 s) | Yes(20 s) | Yes(23 s) |
| Hydrogen Production Rate, moles/s | 0.279 | 0.365 | 0.394 |
| Total Hydrogen Production, moles | 18 | 57 | 54 |
| Maximum Sheath Temperature, °C | 1730 | 1950 | 1870 |
| Maximum Pressure Tube Temp, °C | 1220 | 1310 | 1435 |

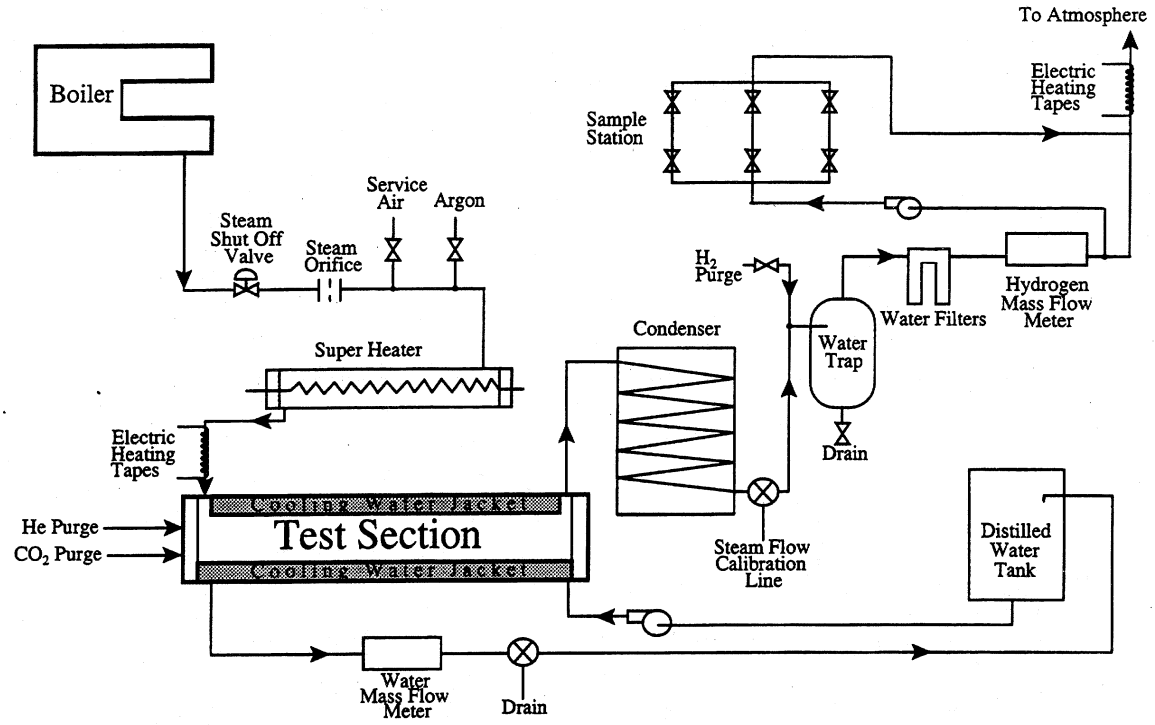


FIGURE 1: SCHEMATIC DIAGRAM OF THE CS28-3 EXPERIMENTAL APPARATUS

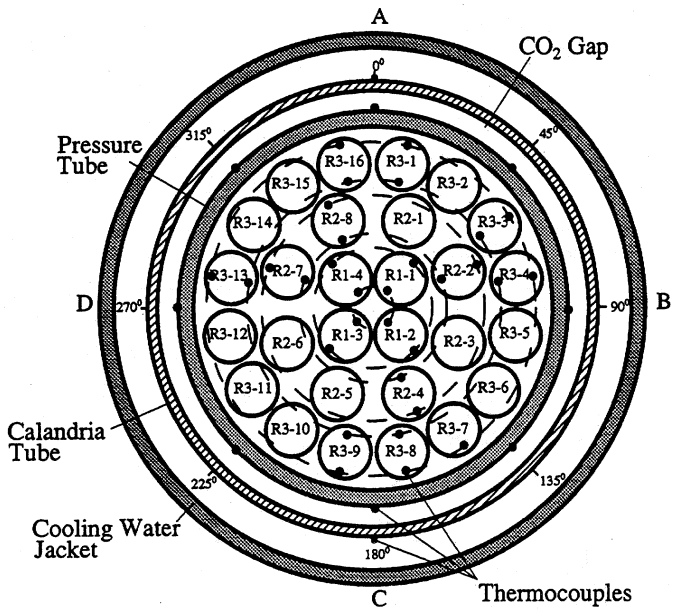


FIGURE 2: CROSS SECTION OF THE CS28-3 TEST SECTION SHOWING THE THERMOCOUPLE RADIAL LOCATIONS

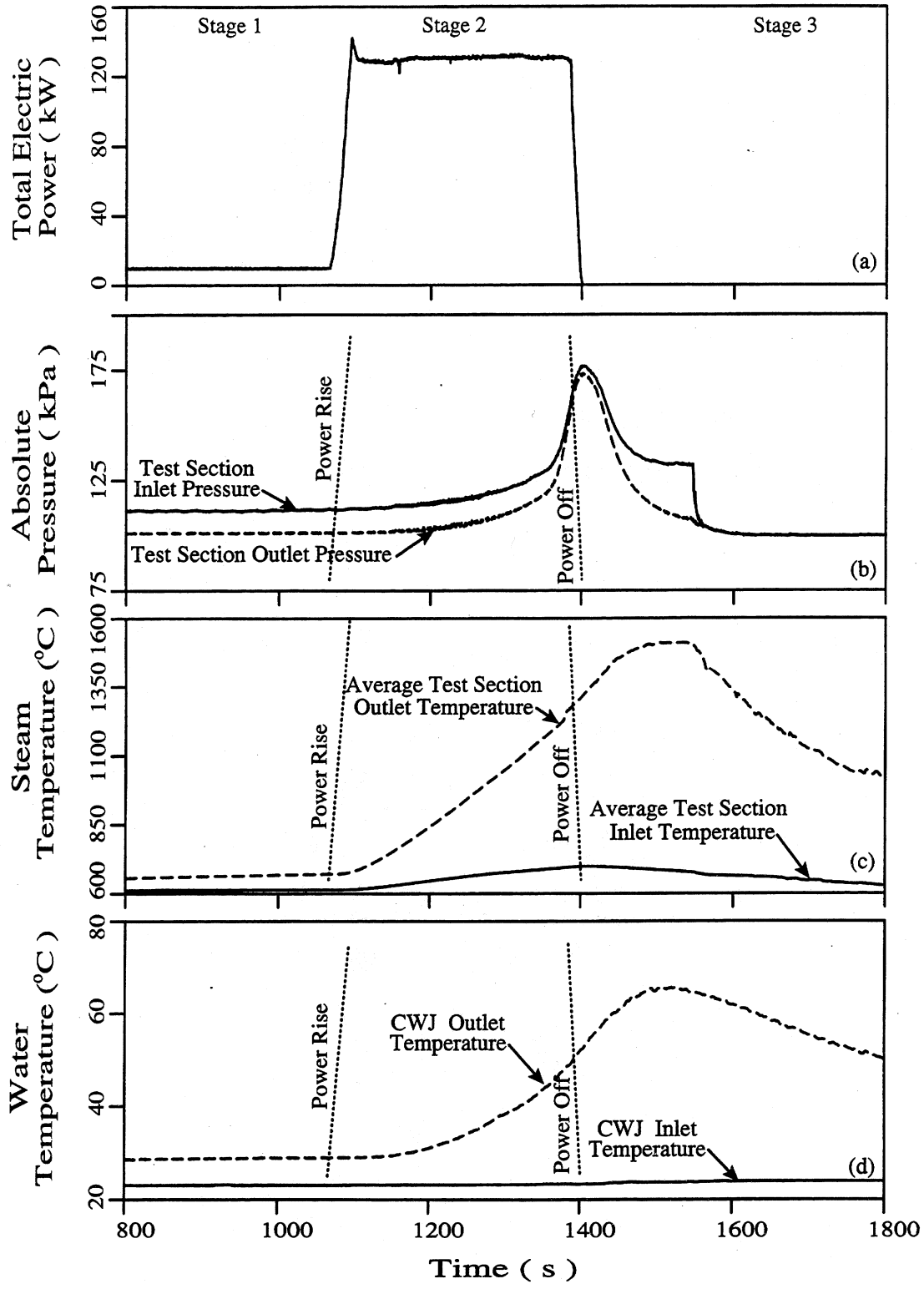


FIGURE 3: HYDRAULIC BOUNDARY CONDITIONS FOR THE CS28-3 TEST SECTION, (a) POWER, (b) PRESSURE, (c) STEAM TEMPERATURE, (d) COOLING WATER JACKET TEMPERATURE

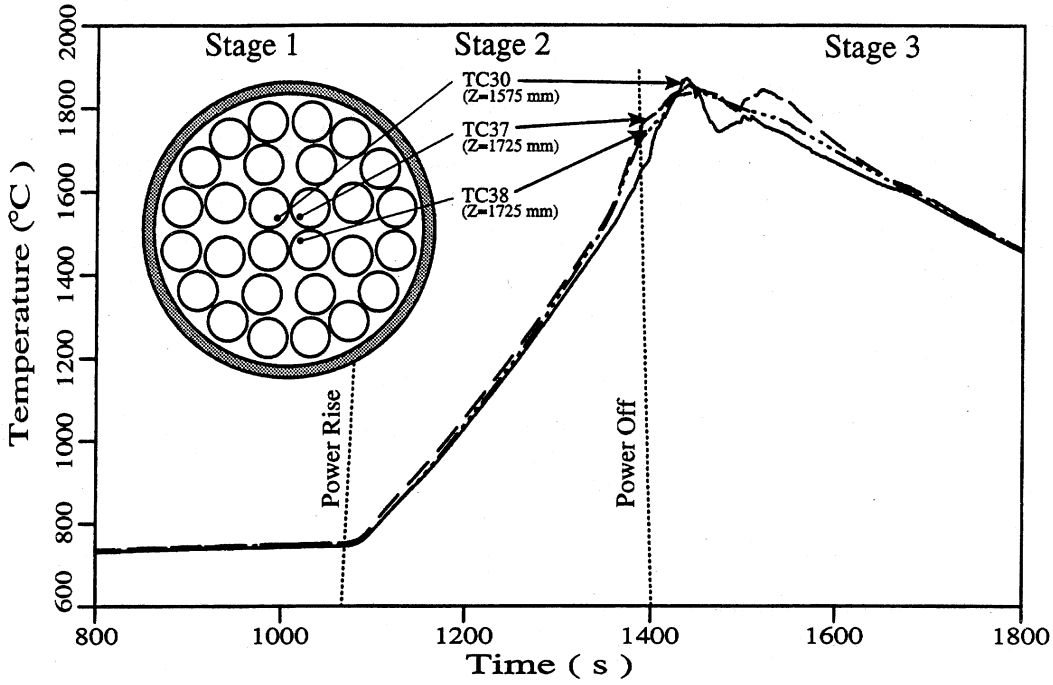


FIGURE 4: HOTTEST FUEL ELEMENT SIMULATOR TEMPERATURES RECORDED DURING THE CHAN CS28-3 EXPERIMENT

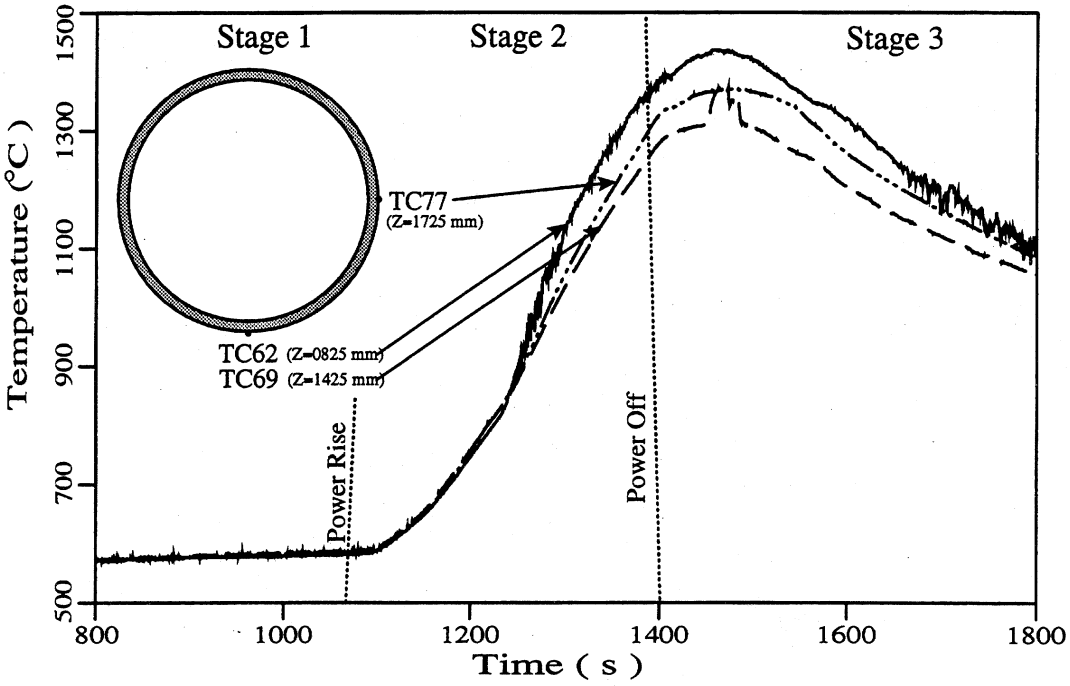


FIGURE 5: HOTTEST PRESSURE TUBE TEMPERATURES RECORDED DURING THE CHAN CS28-3 EXPERIMENT

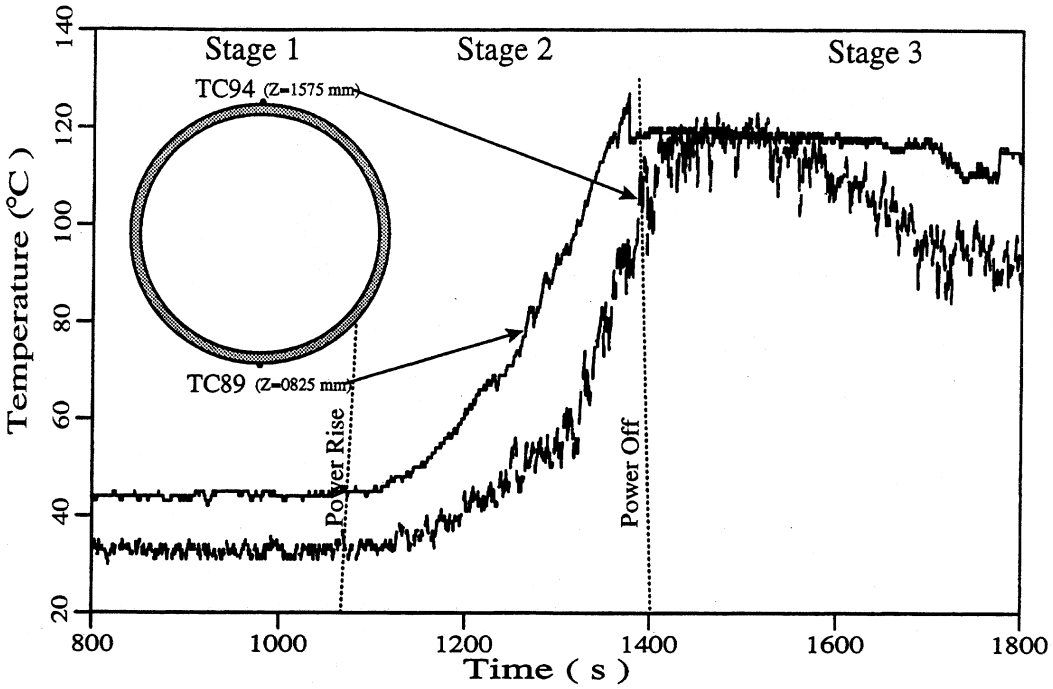


FIGURE 6: HOTTEST CALANDRIA TUBE TEMPERATURES RECORDED DURING THE CHAN CS28-3 EXPERIMENT

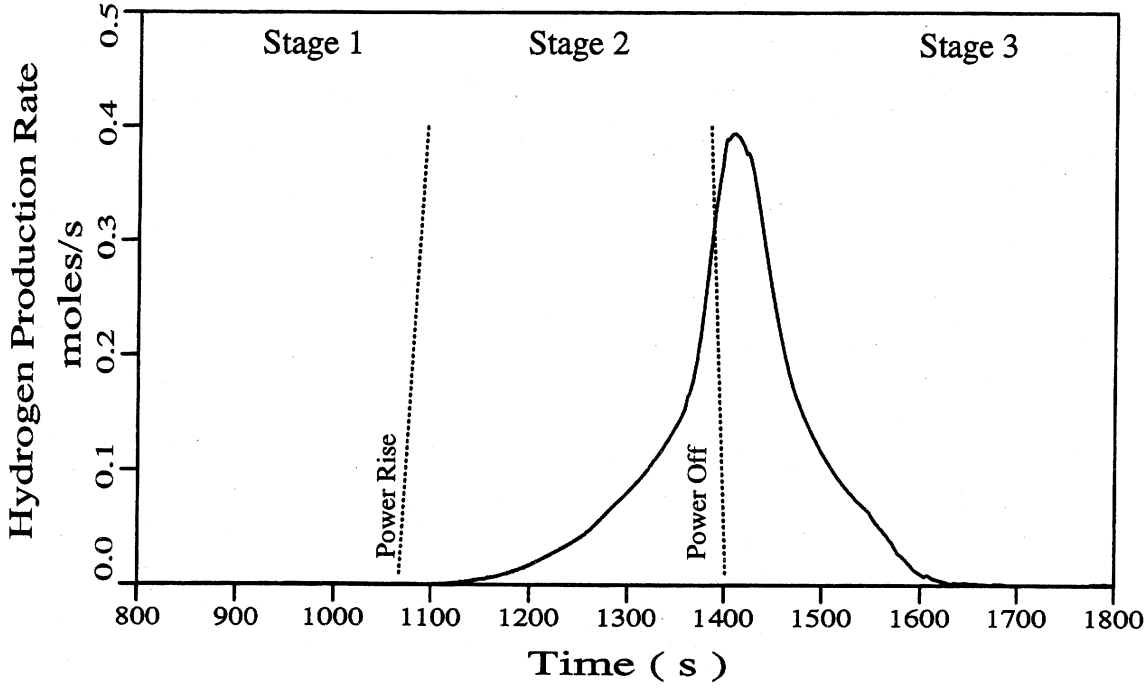


FIGURE 7: HYDROGEN PRODUCTION RATES DURING THE CHAN CS28-3 EXPERIMENT

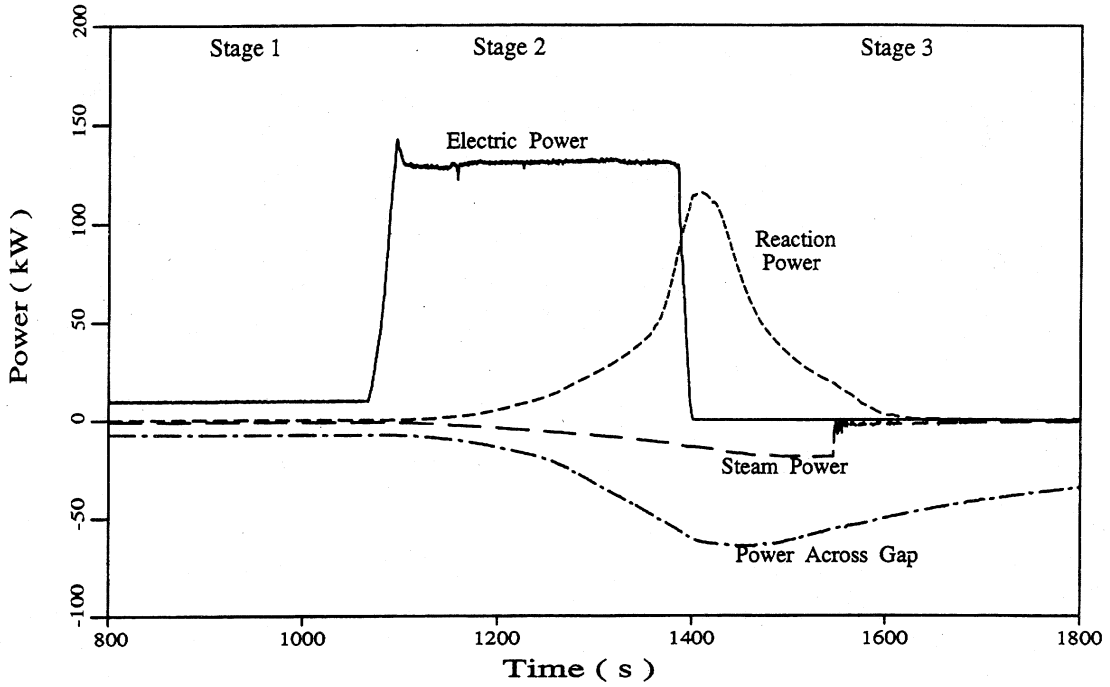


FIGURE 8: COMPONENTS OF THE TEST-SECTION ENERGY BALANCE FOR THE CHAN CS28-3 EXPERIMENT

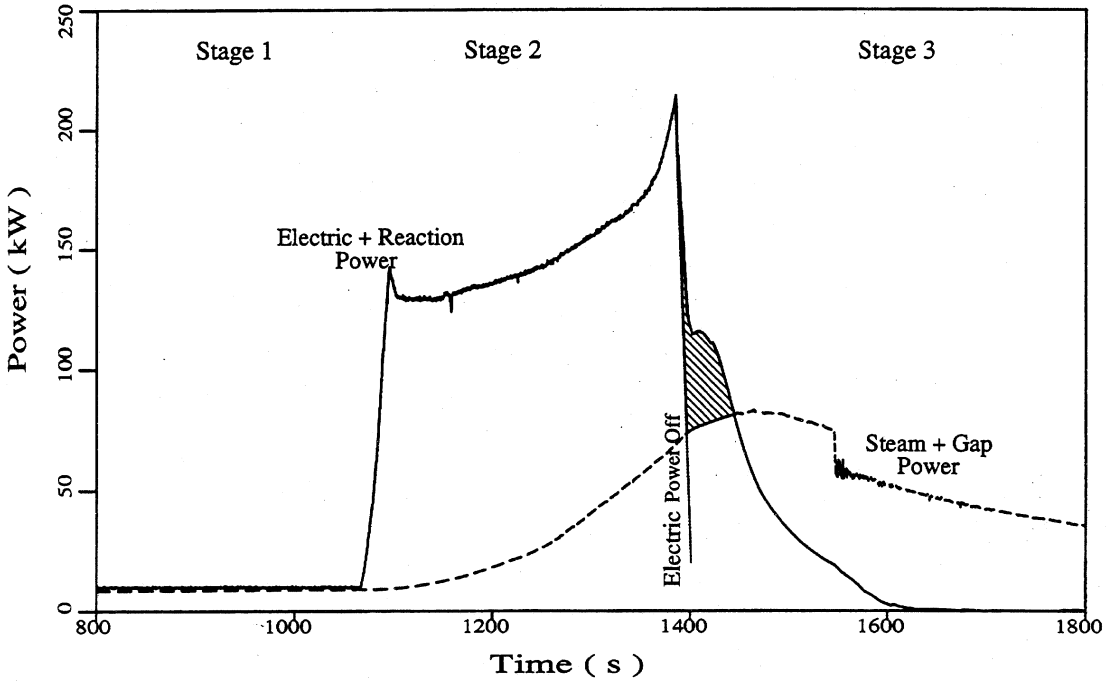


FIGURE 9: OVERALL ENERGY BALANCE OF THE CS28-3 TEST SECTION

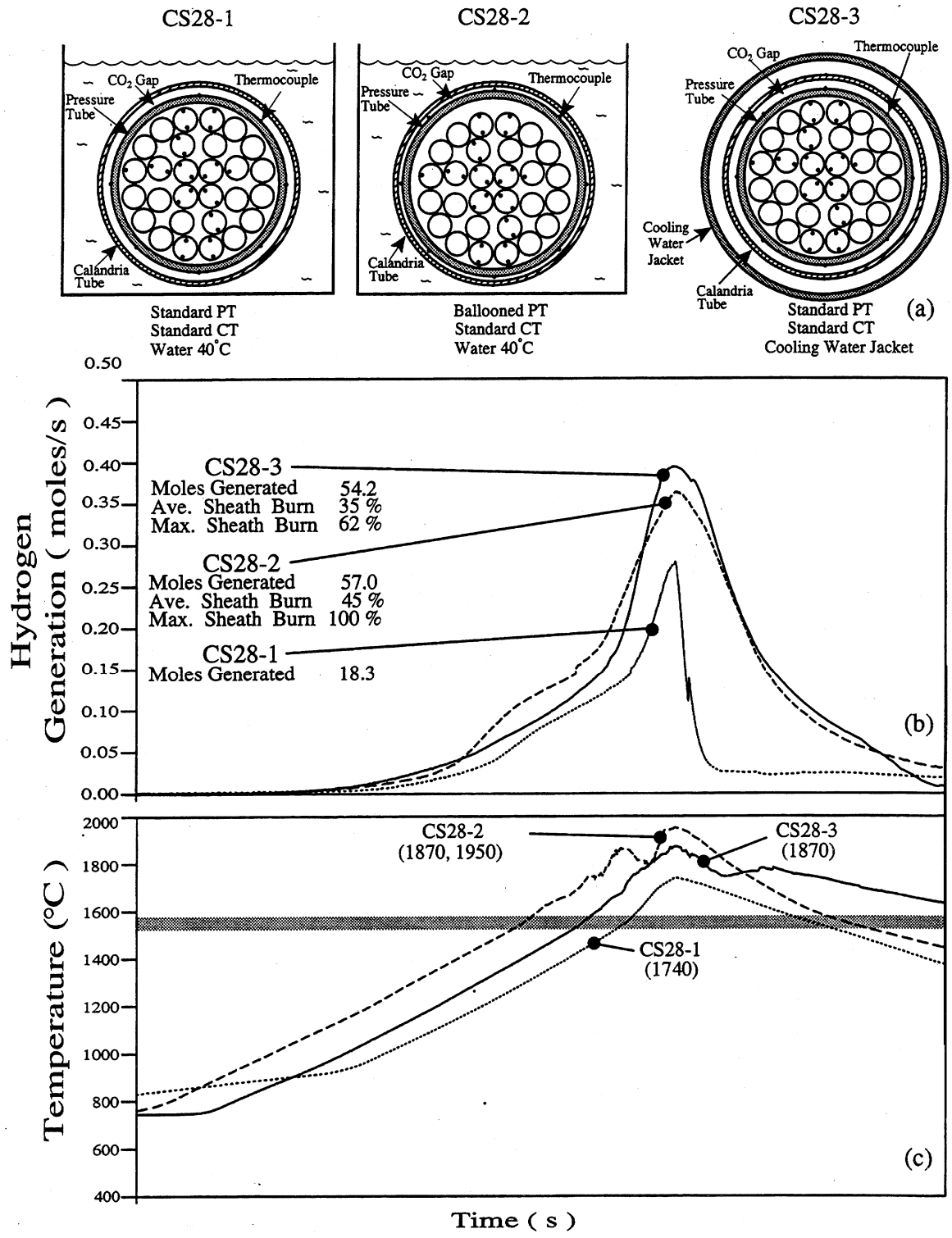


FIGURE 10: COMPARISON OF 28-ELEMENT EXPERIMENTAL RESULTS, (a) TEST SECTION GEOMETRIES, (b) HYDROGEN GENERATION RATES, (c) MAXIMUM RECORDED FES TEMPERATURES

CONFERENCE

FREDERICTON, N. B.

*June 9-12, 1996*

# CNS PROCEEDINGS
# SNC COMPTE RENDU

## VOLUME 2

*17th Annual Canadian Nuclear Society Conference*

*17e Colloque Annuelle de la Société Nucléaire Canadienne*

*Fredericton, New Brunswick*
*Canada*

*Entering the Golden Age*

*A l'aube de l'âge d'or*